Available online at www.sciencedirect.com
ScienceDirect
Ceramics International 38S (2012) S439–S442
CERAMICS INTERNATIONAL
www.elsevier.com/locate/ceramint

Magnetoresistance properties of $0.99La_{0.7}(Ca_xSr_{1-x})_{0.3}MnO_3/0.01CuZnFe_4O_4$ composites

Jin Long Bian, Yong Jun Seo, Geun Woo Kim, Chang Hoon Sung, Shalendra Kumar, Chan Gyu Lee, Bon Heun Koo *

School of Nano & Advanced Materials Engineering, Changwon National University, Changwon 641-773, Republic of Korea

Available online 13 May 2011

Abstract

The composites of $0.99La_{0.7}(Ca_xSr_{1-x})_{0.3}MnO_3/0.01CuZnFe_4O_4$ (LCSMO/CZF) ($x = 0$, 0.1, 0.2, 0.3, 0.5, 0.7 and 1) were fabricated by conventional solid state reaction method, and their electrical transport and magnetoresistance (MR) properties were investigated by physical property measurement system (PPMS). The result of X-ray diffraction (XRD) and scanning electronic microscopy (SEM) indicated that no new phase appeared in the composites except LCSMO and CZF phases. CZF is mainly distributed at the grain boundaries and surfaces of the matrix. The resistivity of all the composites was measured in the range 100–350 K at 0 T, 0.5 T and 1 T magnetic field. Room temperature MR peak appears for the composites $x = 0.03$. The observed variation of MR with varying Ca and Sr concentration has been qualitatively.

Keywords: B. Grain boundaries; C. Magnetic properties; Magnetoresistance; Electrical transport

1. Introduction

Perovskite manganites $L_{1-x}A_xMO_3$ (A = Ca, Sr, Ba) [1] have attracted much attention due to its colossal magnetoresistance (CMR) [2] which has potential application in high speed electronic, magnetic and recording devices, etc. However, the intrinsic CMR in perovskite manganites only can be found within a narrow temperature range around the ferromagnetic–paramagnetic transition temperature at high magnetic field of several teslas, which is incapable for practical application. Since many investigations have been studied, another type of MR effect which is called extrinsic MR effect in polycrystalline manganites has been found. This extrinsic MR is larger and can be found over a wide temperature range at only very low magnetic field. Spin polarized tunneling [3] or spin dependent scattering among neighboring grains seems to be responsible for this kind of MR effects. The introduction of high resistivity second phase in the manganites has a barrier effect to the tunneling process and also causes the magnetic disorder [4] near the grain boundary [5,6]. Hence as the tunneling process is influenced, an enhancement of the magnetoresistance is obtained.

Recently, some attempts have been made to study this enhancement in MR through the formation of composites of $La_{0.7}Ca_{0.3}MnO_3$ (LCMO)/$NiFe_2O_4$, LCMO/$CuFe_2O_4$, $La_{0.7}Sr_{0.3}MnO_3$ (LSMO)/CeO_2, LCMO/$SrTiO_3$, etc. [7–10]. In these systems, nonmagnetic insulators as a second phase were introduced to the perovskite manganites matrix where to form local spin disorder.

LCMO and LSMO are two well-studied manganites among the large number of pure CMR material studied so far. In the present work, we select $La_{0.7}(Ca_xSr_{1-x})_{0.3}MnO_3$ (LCSMO) as the matrix which is a mixture of LCMO and LSMO. According to our research, the Curie temperature (T_c) of LCMO and LSMO are 250 K and 360 K, respectively. When the Ca content x changes, MR at a different transition temperature T_c will be obtained, including room temperature MR. $CuZnFe_4O_4$ (CZF) is selected to be the second phase which has large resistivity and strong ferromagnetic property. The investigation on magnetic properties of LCSMO/CZF has been done. We intend to obtain enhanced MR at room temperature.

* Corresponding author. Tel.: +82 55 264 5431; fax: +82 55 262 6486.
E-mail address: bhkoo@changwon.ac.kr (B.H. Koo).

0272-8842/$36.00
doi:10.1016/j.ceramint.2011.05.029

2. Experimental

The $0.99La_{0.7}(Ca_xSr_{1-x})_{0.3}MnO_3/0.01CuZnFe_4O_4$ ($x = 0$, 0.1, 0.2, 0.3 0.5, 0.7 and 1) composites were prepared by two steps. Firstly, LCSMO powders were fabricated by a two step heating process. The stoichiometric amount of La_2O_3, CaO, SrO and Mn_2O_3 raw powders were mixed completely by ball-milling and grinding process and then pre-calcinated at 1000 °C for 10 h. After calcination the powders were again ball-milled and grinded, and finally sintered at 1250 °C for 24 h. Secondly, the obtained LCSMO fine powders were mixed with high purity CZF. Then the above procedure was done again to obtain the expected composites. Finally, the obtained homogenous LCSMO/CZF composites powders were pelletized into rectangular blocks at the press of 10 MPa. For the final sintering temperature we also chose 1250 °C which is a little higher than the melting temperature of LCSMO and lower than that of CZF.

The distribution of CZF in the matrix was analyzed with a JSM-5610 scanning electron microscopy (SEM). The crystal structure of the resulting samples was checked by a Lab centre XRF-1800 X-ray diffraction (XRD) equipment using Cu Kα radiation at room temperature. The electrical transport behaviors were measured by standard four-probe method by using a quantum design physical property measurement system (PPMS) over a temperature range of 100–350 K.

3. Results and discussion

Fig. 1 shows the XRD patterns of the composites LCSMO/CZF at room temperature. With increasing x from 0.1 to 0.7, it shows that the peak intensity of LSMO phase decreases systematically. At $x = 0.1$ the LSMO peak appears as the main peak of the composite, however when the Ca content gets high to $x = 0.7$, LSMO peaks almost disappear and LCMO peak becomes to be the main peak. Except the LCMO and LSMO patterns, there is also another phase which is CZF. Due to the content of CZF 0.01 is too low that the peaks are not obvious. The results indicate that CZF and LCSMO co-exist in the studied composites. There was no chemical interaction during the sintering process. Considering our experimental procedure, before mixing with CZF, a LCSMO-perovskite structure has been formed. Then during the mixing process, the introduced CZF is preferentially segregated from the LCSMO matrix grains.

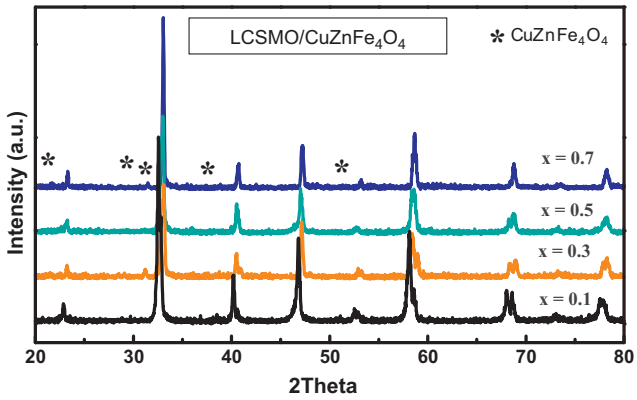

Fig. 1. XRD patterns for selected samples of LCSMO/CZF with $x = 0.1$, 0.3, 0.5 and 8.7.

Fig. 2 gives four representative SEM photographs for pure LCMO, LSMO and LCSMO/CZF $x = 0.3$ and 0.5 composites, respectively. From the images the pure LCMO and LSMO only

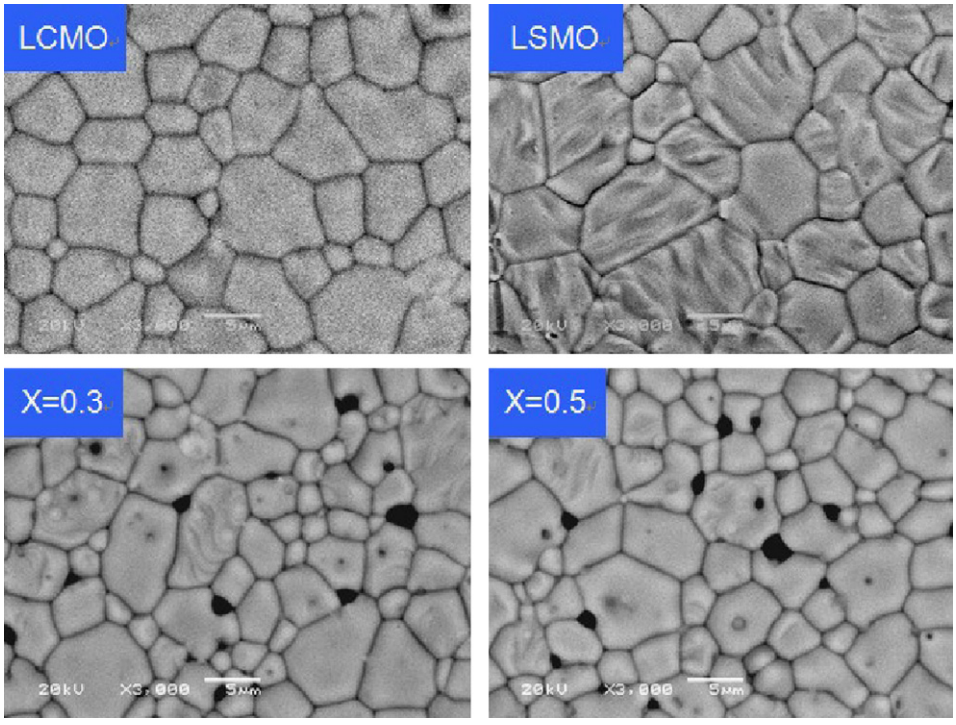

Fig. 2. Scanning electron micrographs of pure LCMO, LSMO and LCSMO/CZF $x = 0.3$ and 0.5.